MISCELLANEOUS PAPER NO. 1-808

WATER SHOCK WAVES FROM ABOVE-WATER EXPLOSIONS

by

J. M. Pinkston, Jr.
Akira Sakurai

March 1966

U. S. Army Engineer Waterways Experiment Station
CORPS OF ENGINEERS
Vicksburg, Mississippi

MISCELLANEOUS PAPER NO. 1-808

WATER SHOCK WAVES FROM ABOVE-WATER EXPLOSIONS

by

J. M. Pinkston, Jr.

Akira Sakurai

March 1966

U. S. Army Engineer Waterways Experiment Station

CORPS OF ENGINEERS

Vicksburg, Mississippi

ARMY-MRC VICKSBURG, MISS.

1

TA7
W34m
no.1-808

Foreword

This paper was prepared for presentation at the 1966 Army Science Conference at West Point, New York. It was approved for presentation and publication by the Office, Chief of Engineers. The paper was prepared by Mr. J. M. Pinkston, Jr., and Dr. Akira Sakurai, under the general supervision of Mr. G. L. Arbuthnot, Jr., Acting Chief, Nuclear Weapons Effects Division, and Mr. J. N. Strange, Chief, Engineering Research Branch, U. S. Army Engineer Waterways Experiment Station.

Director of the Waterways Experiment Station during the preparation of this paper was Col. John R. Oswalt, Jr., CE. Technical Director was Mr. J. B. Tiffany.

TITLE: Water Shock Waves from Above-Water Explosions

J. M. PINKSTON, JR., AND AKIRA SAKURAI
U. S. Army Engineer Waterways Experiment Station
Vicksburg, Mississippi

ABSTRACT:

In an effort to determine the amount of energy transmitted into the water when an explosion occurs above a water surface, both experimental and theoretical investigations were conducted. The experimental study involved detonation of 21-lb spheres of TNT above a water surface and measuring induced water shock at spatial positions underwater. To fully incorporate the nonlinear characteristics of the airblast into the study, free-air pressure-time data were used as the water surface loading mechanism and the investigation was divided into two phases--in Phase I the generating source was at such a height that the induced water shock could be adequately described by acoustic theory, while in Phase II the generating source was nearer the surface and the resulting disturbance field was of a finite amplitude that had to be considered to accurately determine underwater pressure.

Peak pressures and pressure-time histories derived during Phase I (acoustic theory) compare very well with experimental results for those cases wherein the theory is valid. When the generating source nears the surface however, the theory becomes inadequate (primarily because of a rigid interface assumption) and theoretical results are adjusted by a correction factor (θ) that modifies the pressure values as θp. Appropriate θ values for each charge position were obtained by comparing theoretical and experimental results for each charge position.

Phase II results (the effect of the finite disturbance) indicated that the disturbance is not as important as originally estimated, and except near the zero point, the acoustic theory can offer a complete description of the pressure phenomena in water. However, near the zero point, the finite disturbance effect is essential to an accurate determination of the underwater pressure.

BIOGRAPHY:

PRESENT ASSIGNMENT: Supervisory Research Physicist, U. S. Army Engineer Waterways Experiment Station

DEGREES HELD: Bachelor of Science, Millsaps College, Jackson, Mississippi, 1956.

developed during the investigation would be in such a form that the numerical procedure to determine the pressure-time history at spatial positions underwater could be easily performed.

The theoretical investigation was divided into two phases. In Phase I it was assumed that the generating source was at such a height above the surface that the induced water shock could be adequately described by acoustic theory, while Phase II covered those cases in which the generating source was nearer the surface and the resulting disturbance field in water was of a finite amplitude that had to be considered in determining underwater pressure.

PHASE I - ACOUSTIC THEORY

In this phase of the investigation the problem can be reduced to that of finding the pressure field (p) in the water from the wave equation, subject to the boundary condition given by the pressure loading p_0 on the surface. Assuming p_0 as

$$p_0(r,t) = \begin{cases} a_0(t) + r^2 a_1(t) + r^4 a_2(t) + \ldots, & \text{for } R \geq r \geq 0 \\ 0 & \text{for } r > R \end{cases} \tag{1}$$

(see Figure 1)

where $a_0(t)$, ..., are functions of time (t), the general solution for p can be simplified into an expression given by a series of single integrals including $a_0(t)$, $a_1(t)$, ..., in each integral as

$$p(r,z,t) = p_0\left(r,t - \frac{z}{c}\right) H\left[R\left(t - \frac{z}{c}\right) - r\right] + \sum_{n=0}^{\infty} \int_{t_1(r,z,t)}^{t_2(r,z,t)} f_n(r,z,t,t')a_n(t')dt' \tag{2}$$

where H is the Heaviside function and f_n are known functions of r , z , t , and t' (z = gage depth). The limits t_1 and t_2 are functions that are determined for each gage location (r,z) and time t .

The $a_0(t)$, ..., functions were determined using both experimental free-air pressure-time data and the properties of a reflected airblast wave at a rigid interface. Although practically any number of these functions can be determined, indications are that when compared with experimental data sufficient accuracy is obtained using only the second approximation, i.e. retaining just the $a_0(t)$ and $a_1(t)$ terms. These simplifications make it easier to determine the pressure-time history at a given position

underwater by numerical integration over the desired time interval. Peak pressure values were determined directly from Equation 2 using a limiting process. All equations were programmed for computer processing, and the results obtained are compared with experimental data in Figures 2 through 7.

Since the acoustic theory becomes inadequate when the generating source nears the water surface (primarily because of the rigid interface assumption used to determine the $a_0(t)$, ..., functions), theoretical values given by the acoustic theory are not in good agreement with experimental results; however, these theoretical values can be partially adjusted using a correction factor (θ) that modifies the pressure values as θp. Appropriate θ values (which should be in the range of $0 < \theta < 1$) for each charge position were obtained through a formal comparison of theoretical and experimental results as shown in the following paragraphs.

Peak pressure values for the case when the charge is directly above the gages ($\lambda_r = 0$) are plotted (solid lines) in Figure 2. The upper half of the figure illustrates test geometry where λ_H is reduced charge height, λ_r is reduced horizontal distance from charge surface zero to gage surface zero, and z is the gage depth in feet. The two curves for each λ_H correspond to θ values of 0.8 and 1.0. For reduced charge heights of 4λ and 5λ, theoretical and experimental results are in excellent agreement, but as suspected, the theory becomes inadequate as the charge nears the water surface. Figure 2 establishes the range and validity of the present theory and provides an estimate of the appropriate θ value for each charge position. (A θ value of 0.6 when $\lambda_H = 1$ and 0.7 when $\lambda_H = 2$ or 3.)

Figure 3 is a plot of arrival time as a function of gage depth and indicates that the shock wave in water is well documented by acoustic theory. Peak pressure calculations for spatial positions underwater were equally successful when compared with experimental data as shown in Figures 4 and 5 for the illustrated test conditions.

Experimental pressure-time results are compared with theory in Figure 6 for the case when the charge is directly above the gages ($\lambda_r = 0$). The results compare very well, particularly for the deeper gages. Pressure-time histories at spatial positions underwater are contained in Figure 7. Except for an apparent difference in shock wave decay rates for the deeper gages, theoretical and experimental results are in good agreement and further improvements can be expected by retaining additional terms, that is, a_2, a_3, ..., in the basic equation.

PHASE II - THE FINITE DISTURBANCE EFFECT IN WATER

As stated earlier, when the generating source nears the water surface the acoustic theory is no longer valid and the effect of the finite disturbance must be considered. Though the disturbance is of a finite amplitude, it is reasonable to assume that the

disturbance field is restricted to a small region on the water surface. Figure 8 illustrates this particular case which is characterized by the interaction of the airblast and water shock fronts at point c on the water surface. When this occurs, the water is compressed, its front is a genuine shock wave, and a nonlinear analytical approach is required to determine the flow field. Fortunately the flow field near the intersection (point c) acts independently, and its exact solution can be determined through the Rankine-Hugoniot relations of both the air and water shock fronts and knowing the conditions that exist at the interface. These relations are reduced to a system of transcendental equations to determine the angles of intersection, in addition to pressures, velocities, and densities in both the air and water. The equations were solved numerically, and the water shock pressure values obtained for various reduced charge heights are shown in Figure 9. (These values correspond to p_0 values when $r = R$ in Equation 1.)

Table 1 compares p_0 values for $r = R = 0$ from Phase I with corresponding values from Phase II. Since Phase I results are based on the rigid interface assumption, the difference in the two values indicates what effect the compressibility of water has on its reflection characteristics.

TABLE 1

PEAK PRESSURES AT $r = R = 0$ FOR VARIOUS λ_H VALUES

	0.1	0.5	1.0	2.0	3.0	4.0
Phase I	67,390	16,212	6,566	1,872	594	291
Phase II	63,763	15,697	6,432	1,852	591	291

Results show a decrease in pressure that is more pronounced near the water surface. Though the difference is rather small and perhaps insignificant, except for the $\lambda_H = 0.1$ case, these data do suggest that the effect of the finite disturbance in water is not as important as originally estimated.

Using the solution near the point c , a successive approximation method to determine the entire flow field in air and water was developed and its first approximation studied in detail. Figure 10 shows a plot of pressure values from this first approximation for the $\lambda_H = 0.5$, $\lambda_r = 0$ case as compared with available experimental data. Again, indications are that the acoustic theory can offer a complete description of the pressure phenomena in the water, with the exception of the near zero point, if the appropriate θ value is selected. In the vicinity of the zero point, however, the finite disturbance effect in water is essential to an accurate determination of the underwater pressure.

REFERENCES

1. BLAST MEASUREMENTS, Scientific Director's Report Annex 1.6, Operation GREENHOUSE, Part I - Summary Report, WT-64, 1951, CONFIDENTIAL Formerly Restricted Data

2. Thaler, W. J., et al., UNDERWATER PRESSURE MEASUREMENTS, Project 1.4, Operation CASTLE, WT-903, June 1958, SECRET RESTRICTED DATA

3. Thiel, M. A., and Belliveau, L. J., DAMAGE RANGES FOR DETONATION OF PROPELLANT OF POLARIS MISSILE, NAVORD Report 5745, U. S. Naval Ordnance Laboratory, Silver Spring, Maryland, September 1957, SECRET

4. Conway, M. V., INVESTIGATION OF THE CHARACTERISTICS OF AIR-TO-WATER SHOCKS, TN-4868, U. S. Naval Ordnance Laboratory, Silver Spring, Maryland, January 1962, CONFIDENTIAL

5. Lindh, G., SHOCK-WAVE EFFECTS IN WATER IN THE CASE OF DETONATION ABOVE THE WATER SURFACE, Swedish Translation Report No. 25, U. S. Naval Ordnance Laboratory, Silver Spring, Maryland, March 1961, UNCLASSIFIED

6. Lindh, G., TRANSMISSION OF A TRANSIENT SPHERICAL WAVE AT A PLANE INTERFACE, Acustica, Volume 12, Number 2, 1962, pp. 108 through 112, UNCLASSIFIED

7. Bagdoev, A. G., SPATIAL NON-STATIONARY MOTIONS OF A SOLID MEDIUM WITH SHOCK WAVE, Atomic Energy Translation No. 5400, November 1962, UNCLASSIFIED

Security Classification

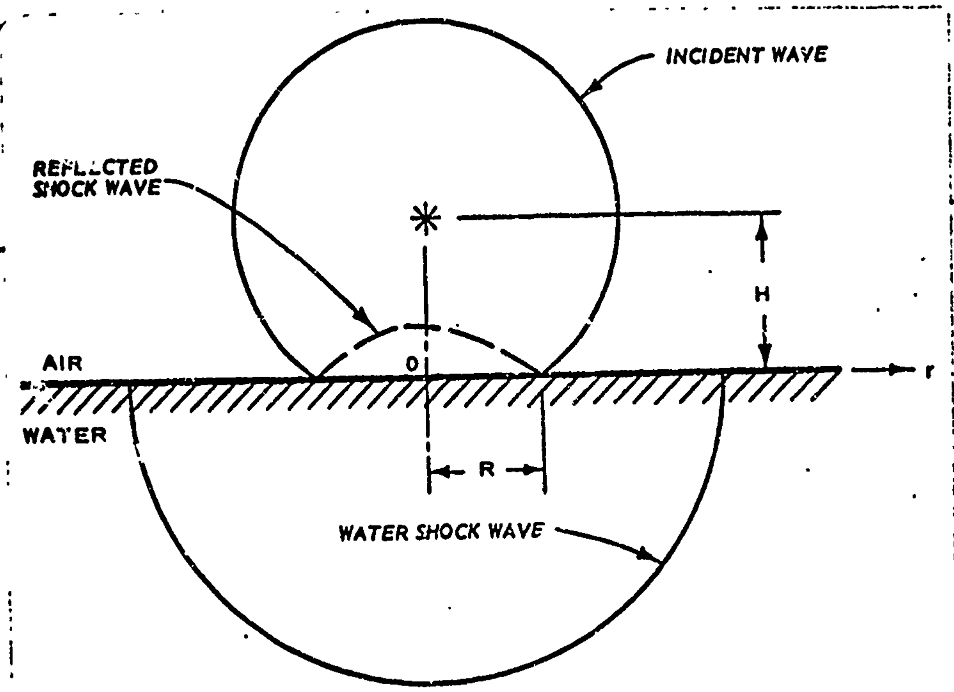

Figure 1. Shock front geometries

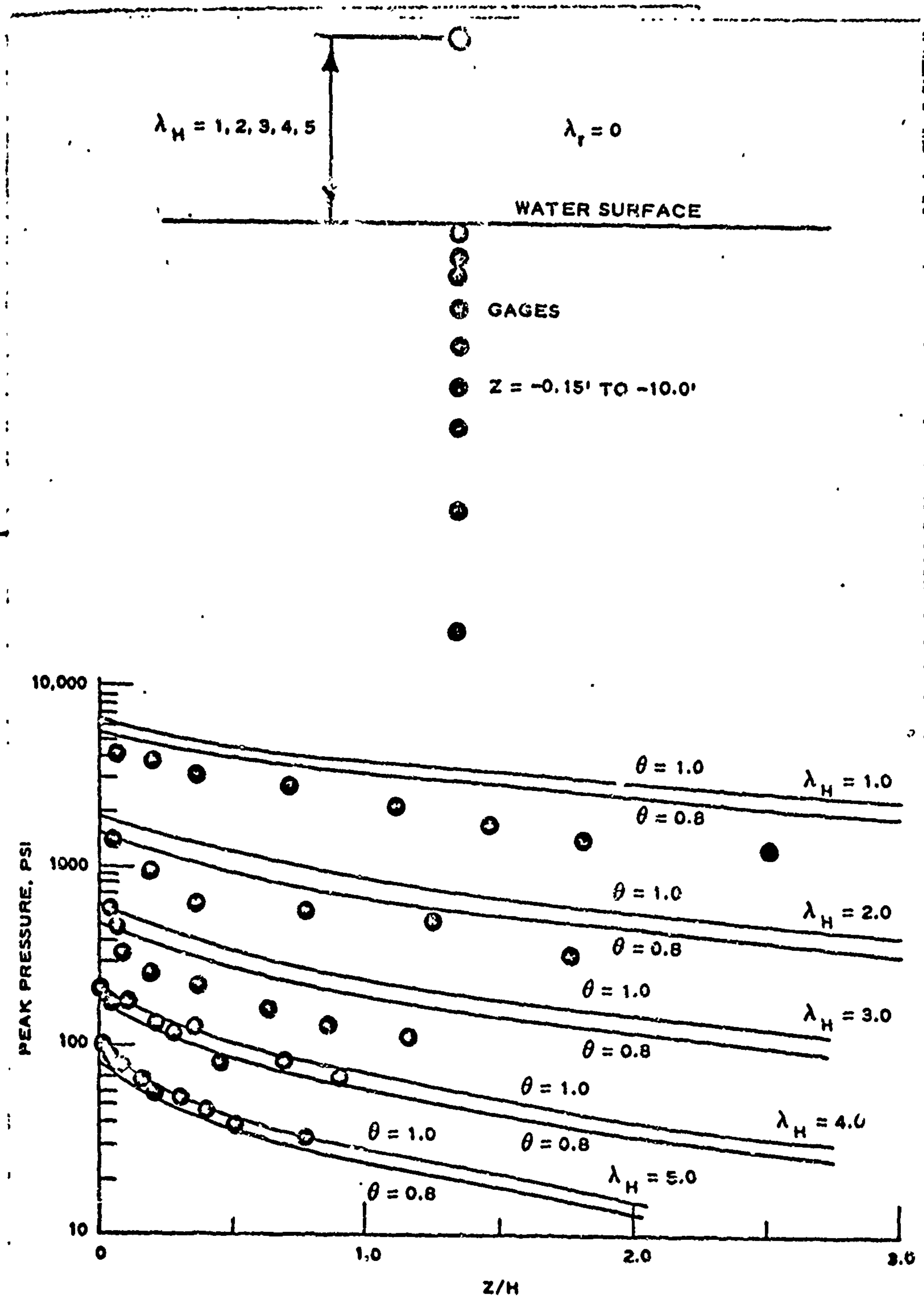

Figure 2. A comparison of theoretical and experimental peak pressure values for different test geometries

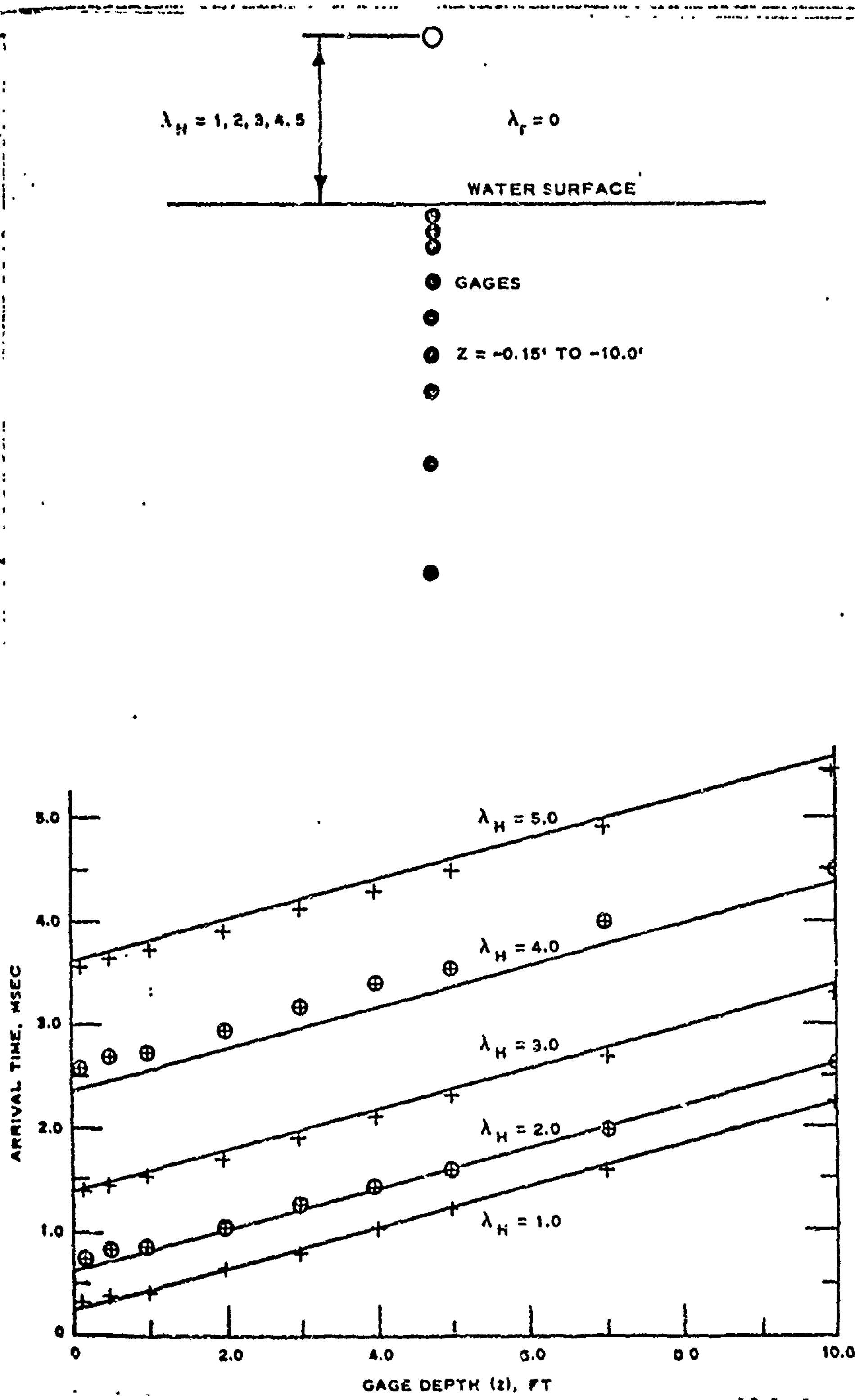

Figure 3. A comparison of theoretical and experimental arrival time values for different test geometries

STAMP Security Classification here

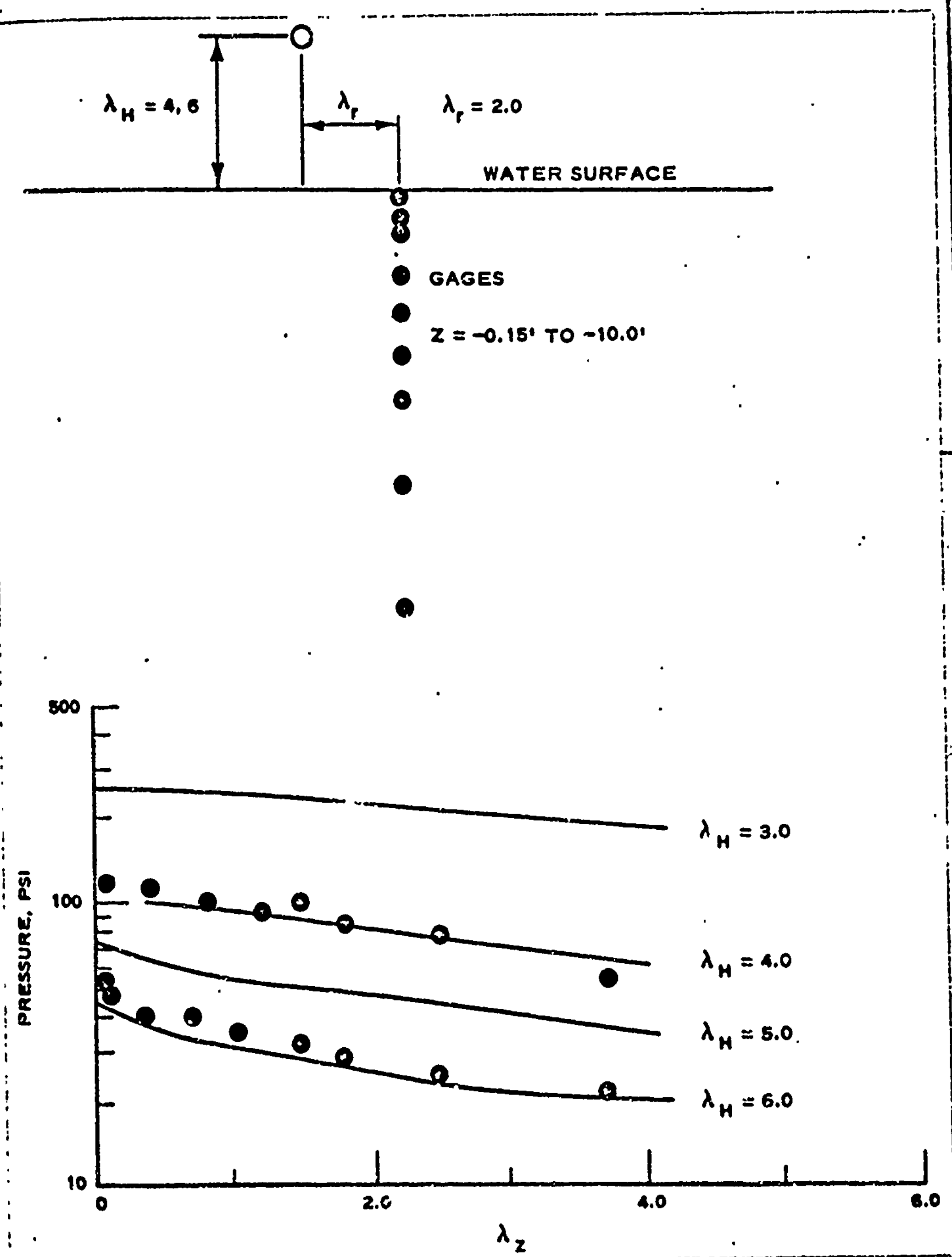

Figure 4. Peak pressure at various gage locations for a reduced horizontal distance (λ_r) of 2

STAMP Security Classification here in black ink

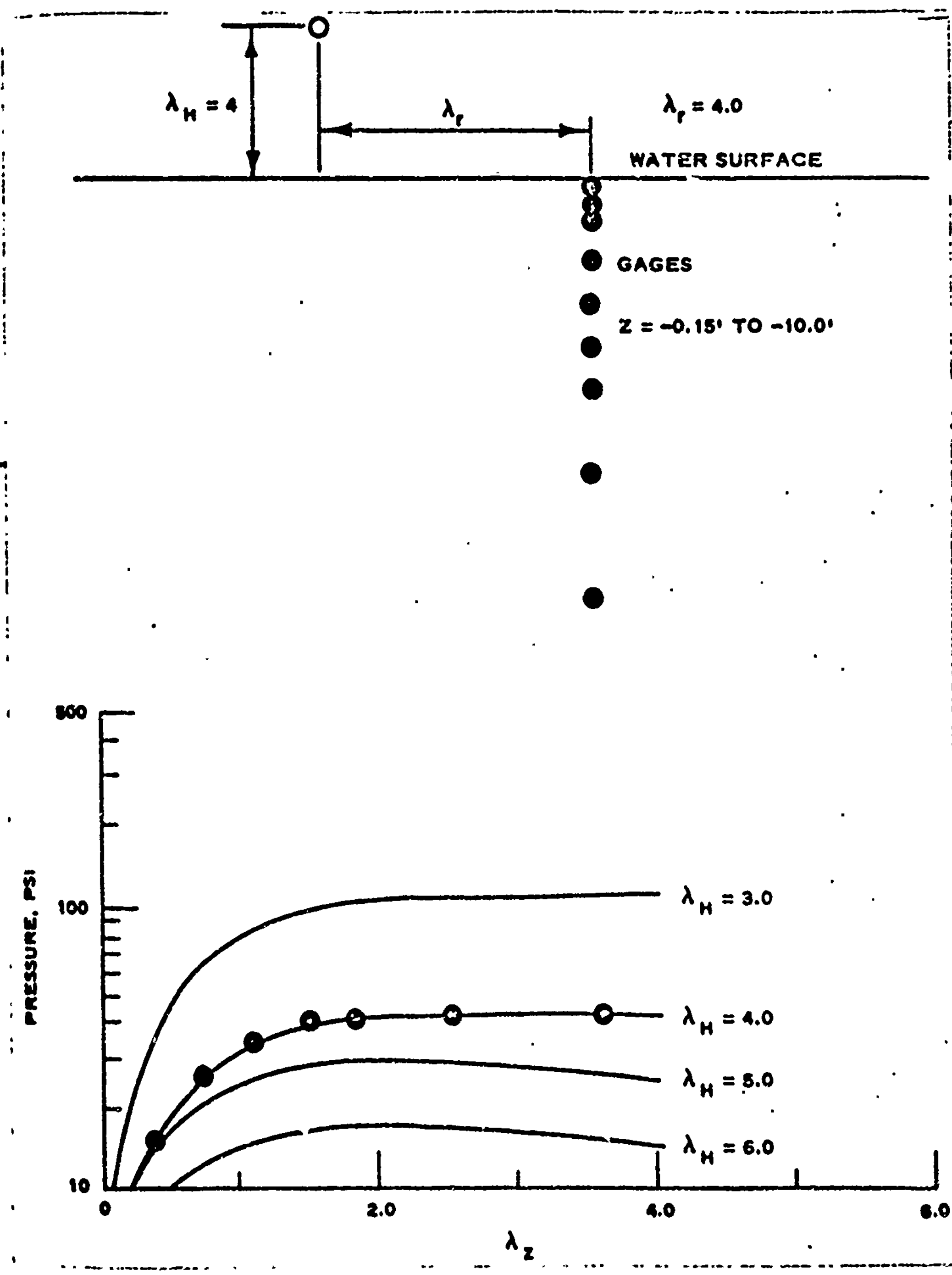

Figure 5. Peak pressure at various gage locations for a reduced horizontal distance (λ_r) of 4

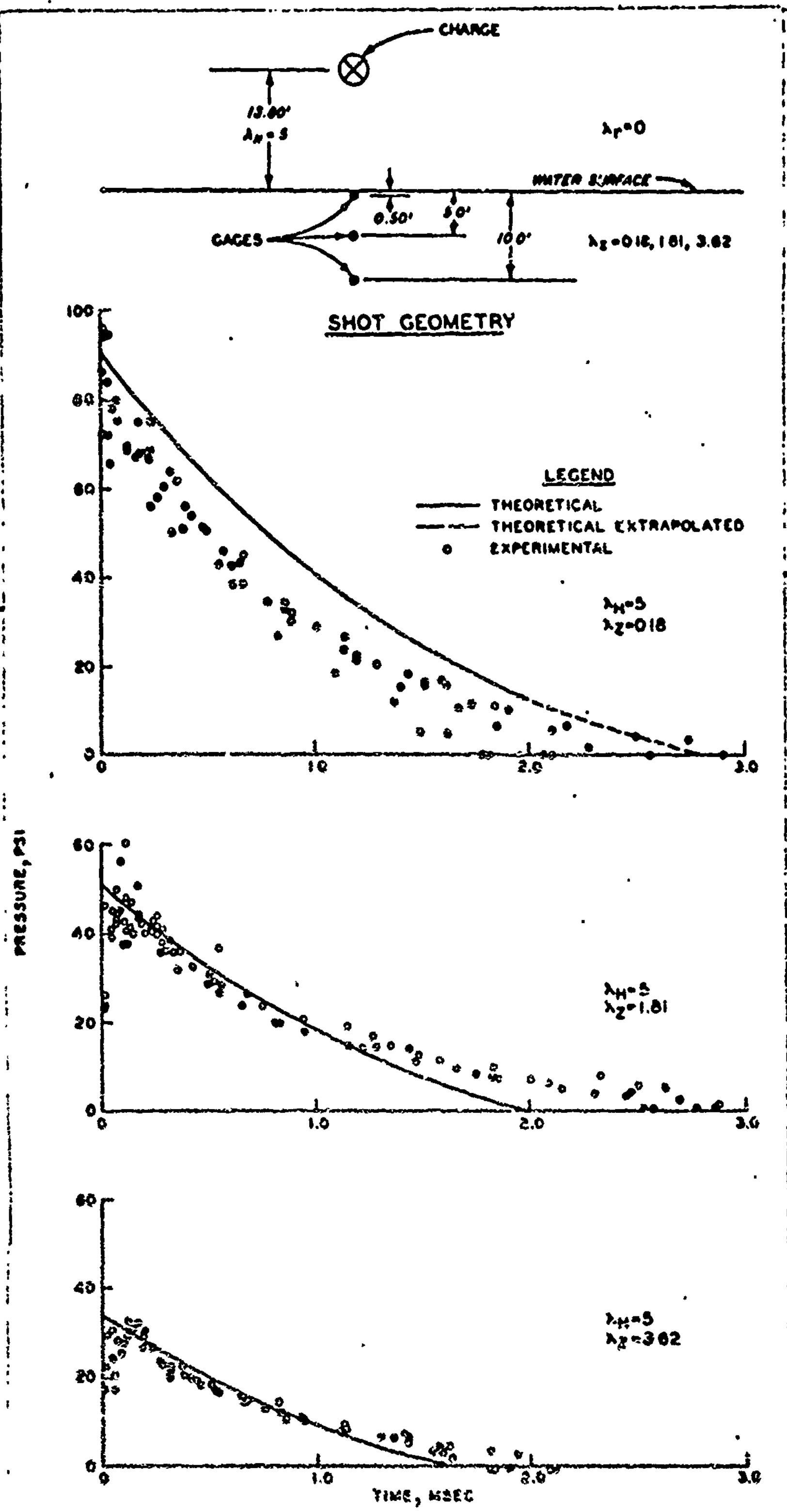

Figure 6. Theoretical and experimental pressure-time histories at various locations for the $\lambda_r = 0$ case

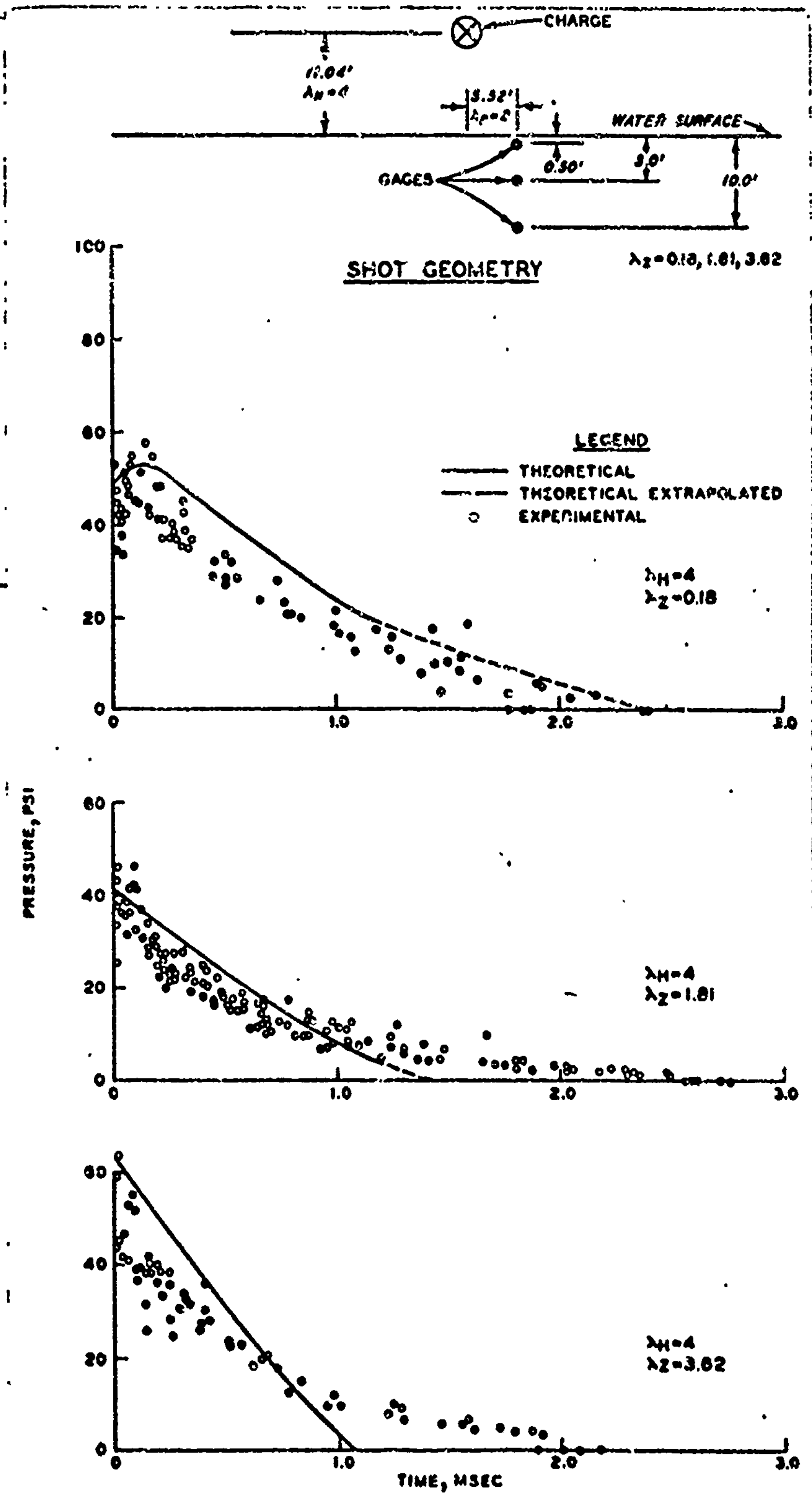

Figure 7. Theoretical and experimental pressure-time histories at various locations for a reduced horizontal distance (λ_r) of 2

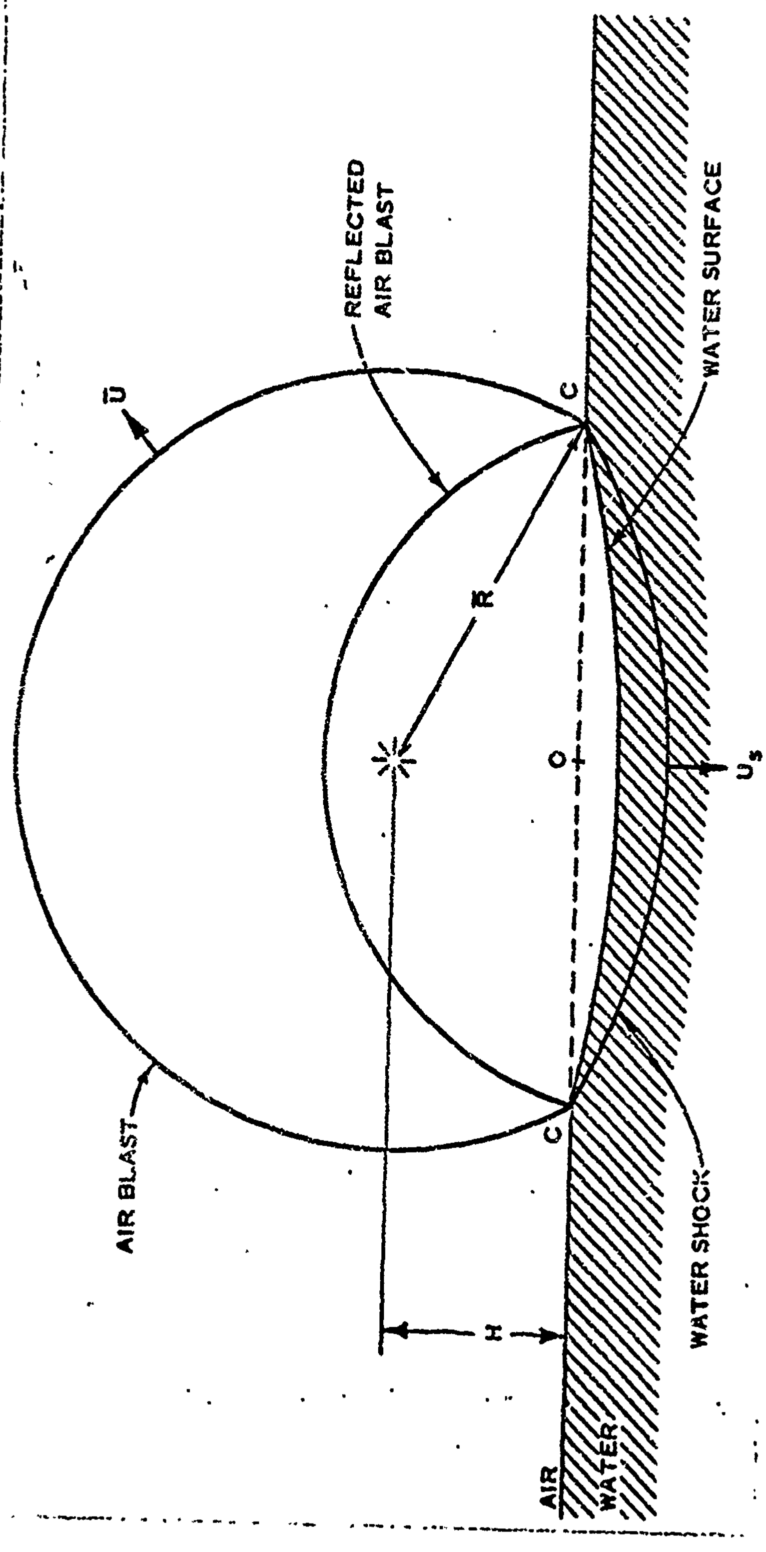

Figure 8. Shock interaction at the water surface illustrating the compressibility of the water

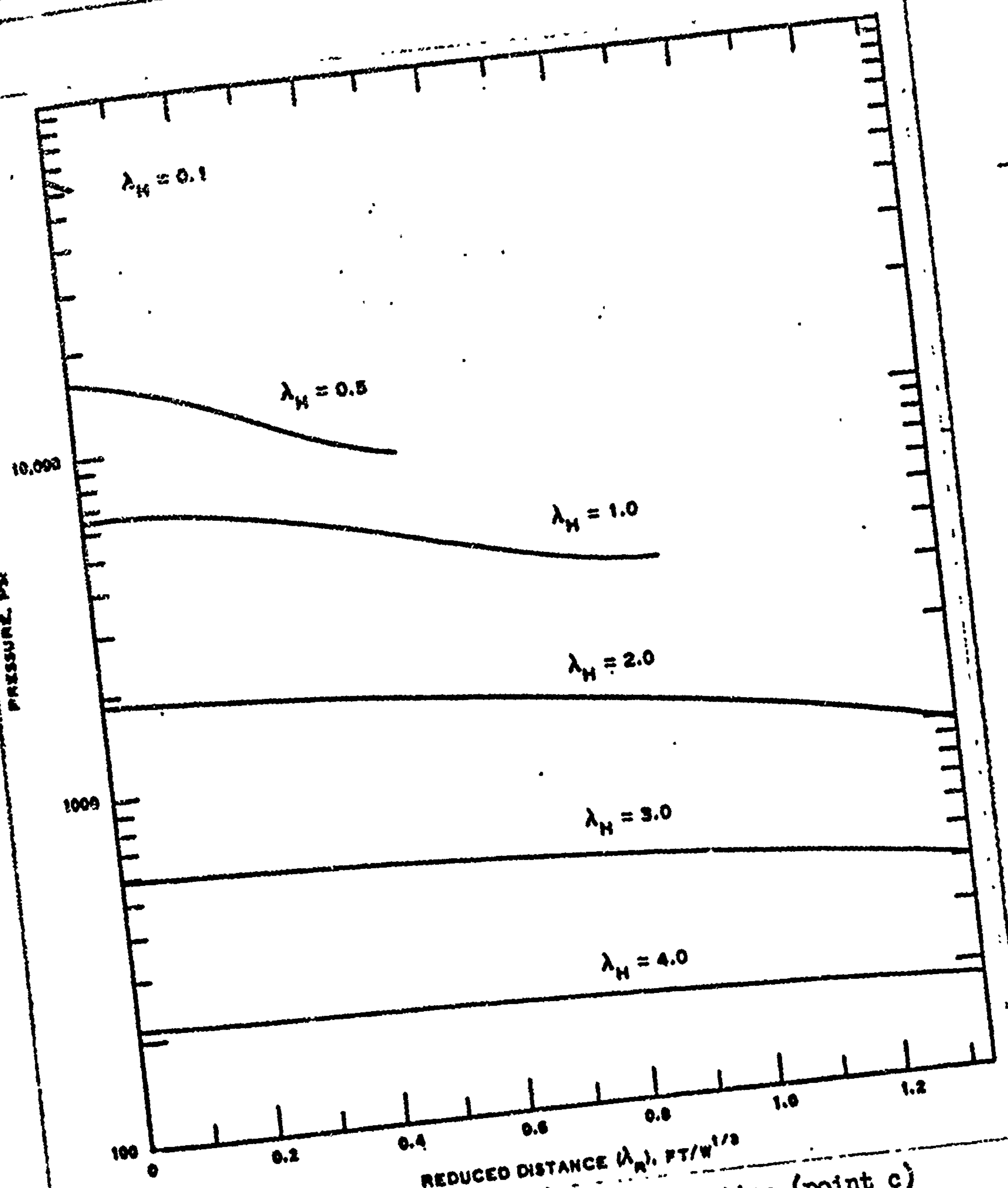

Figure 9. Peak pressure at the intersection (point c) on the water surface

STAMP Security Classification Here

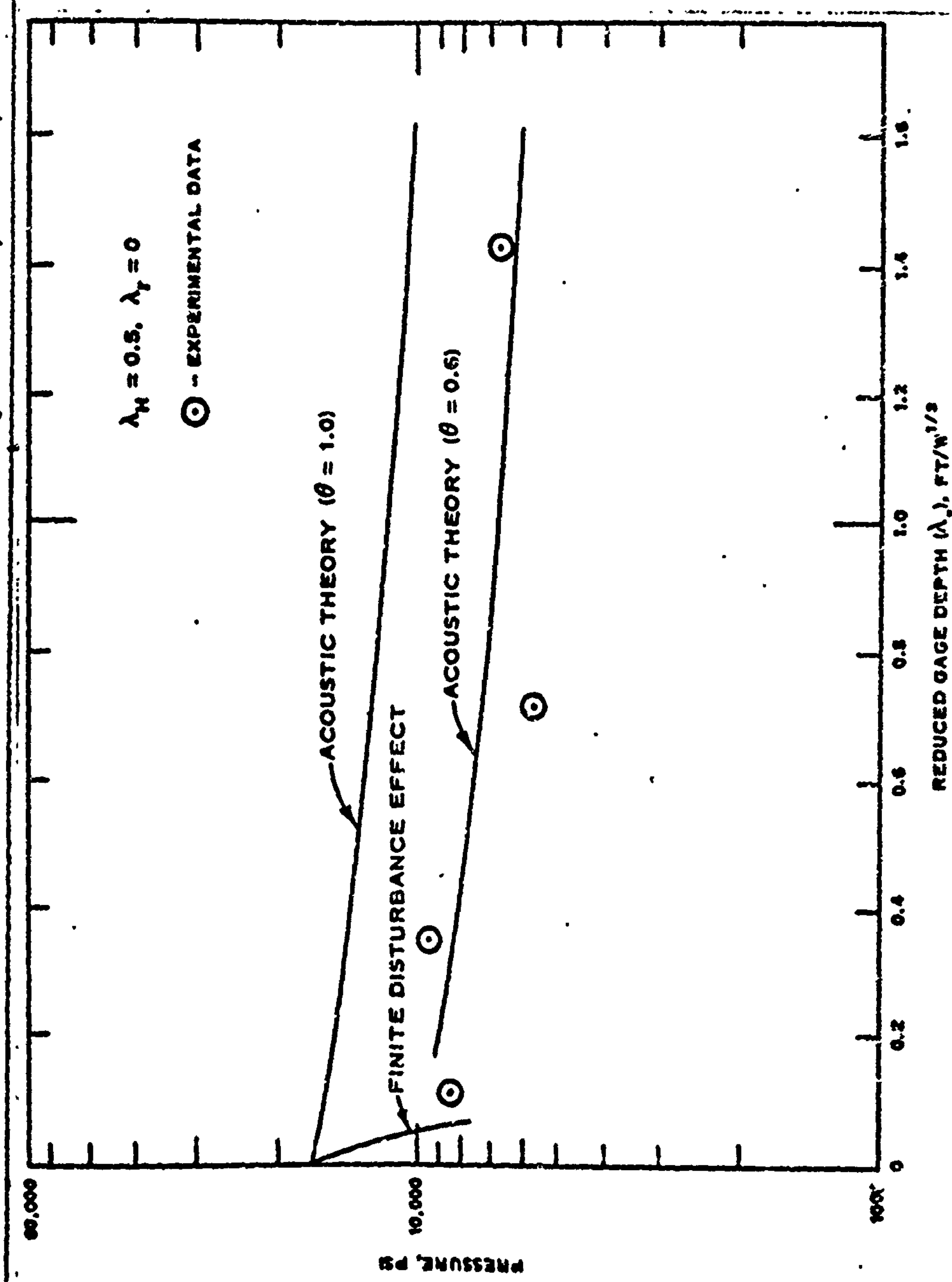

Figure 10. Theoretical results from the linear acoustic theory and the finite disturbance effect in water compared with experimental data

58231